Charge-Based Detection

DOI: 10.1002/ange.201411040

Real-Time Monitoring of Phosphorylation Kinetics with Self-Assembled Nano-oscillators**

Yimin Fang, Shan Chen, Wei Wang, Xiaonan Shan,* and Nongjian Tao*

Abstract: *Phosphorylation is a post-translational modification that is involved in many basic cellular processes and diseases, but is difficult to detect in real time with existing technologies. A label-free detection of phosphorylation is reported in real time with self-assembled nano-oscillators. Each nano-oscillator consists of a gold nanoparticle tethered to a gold surface with a molecular linker. When the nanoparticle is charged, the nano-oscillator can be driven into oscillation with an electric field and detected with a plasmonic imaging approach. The nano-oscillators measure charge change associated with phosphorylation of peptides attached onto a single nanoparticle, allowing us to study the dynamic process of phosphorylation in real time without antibodies down to a few molecules, from which Michaelis and catalytic rate constants are determined.*

Phosphorylation is the addition of a phosphate group to a protein at a specific site assisted with enzymes, namely kinases. This important post-translational modification of proteins is involved in almost all basic cellular processes, including cell metabolism, growth, division, differentiation, motility, and signaling,[1] and is closely related to various diseases, ranging from inflammatory diseases, diabetes, neurodegenerative diseases, and cancers.[2] Detecting and controlling protein phosphorylation are thus critical to understand the basic cellular processes and treat the related diseases.[3] Traditionally, fluorescent-labeled antibodies are used to detect phosphorylation. While useful, this approach requires different antibodies for different phosphorylation sites, and to date antibodies are available for only a small fraction of the potential phosphorylation sites. Western blot[4] and mass spectrometry[5] have also been developed to detect phosphorylation. All these approaches are end point assays, which cannot monitor the dynamic process of phosphorylation and extract important parameters, such as phosphorylation rate in real time. Other technologies, such as surface plasmon resonance (SPR)[6] and quartz crystal microbalance (QCM),[7] can measure molecular binding processes in real time, but they are based on the detection of molecular mass changes, which are difficult to detect phosphorylation that involves a small mass change (ca. 100 Da). For the reasons described above, direct monitoring of phosphorylation has been a challenging task.[8,9]

Herein we report a label-free detection of phosphorylation in real time with self-assembled nano-oscillators. Instead of detecting mass change associated with phosphorylation, the nano-oscillators measure the charge change on each nanoparticle, allowing us to study phosphorylation of a small number of peptide molecules. We have studied the dynamic process of phosphorylation in real time without antibody, from which Michaelis constant and catalytic rate constant are determined. Because an array of nano-oscillators can be self-assembled with a high density, and interrogated individually, the method promises potential high throughput.

The basic principle of the self-assembled nano-oscillator detection platform is illustrated in Figure 1a. Each nano-oscillator consists of a Au nanoparticle anchored to a Au surface with a flexible molecular linker. When the nanoparticle is charged, it can be driven into oscillation by applying an electric potential to the Au surface, and the oscillation amplitude is proportional to the charge on the Au nanoparticle. Using a plasmonic imaging setup,[10] the oscillation amplitude can be determined with an accuracy of 0.1 nm, corresponding to an effective charge of about 0.18 electrons on the nanoparticle.[11] To study phosphorylation, we functionalize the nanoparticles with peptides containing an active tyrosine residue (Supporting Information). Upon introduction of kinase and ATP, a phosphate group is added to the surface-bound peptide, resulting in a change in the charge of the nanoparticle, which is monitored by detecting the oscillation amplitude. By measuring the charge vs. time, the kinetics of phosphorylation on each of the nanoparticles is monitored in real time (Figure 1b).

The detection principle can be more precisely described by analyzing the equation of motion of the nano-oscillators given by Equation (1):[11]

$$m\frac{d^2x}{dt^2} = -kx - 6\pi\eta a\frac{dx}{dt} + qE_0\cos(2\pi ft) \quad (1)$$

where x, m, a, and q are the vertical displacement, mass, radius, and effective charge of the nanoparticle, respectively, k is the spring constant of the molecular linker, and E_0 and f are the amplitude and frequency of the applied electric field, respectively. In the present work, the biotin-PEG molecular

[*] Y. Fang, S. Chen, Prof. W. Wang, Prof. N. Tao
State Key Laboratory of Analytical Chemistry for Life Science
School of Chemistry and Chemical Engineering
Nanjing University, Nanjing 210093 (China)
E-mail: wei.wang@nju.edu.cn
X. Shan, Prof. N. Tao
Center for Bioelectronics and Biosensors
Biodesign Institute, Arizona State University
Tempe, AZ 85287 (USA)
E-mail: xshan2@asu.edu

[**] We thank financial support from the National Natural Science Foundation of China (NSFC, Grant No. 21327008, 21405080, 21327902), the Natural Science Foundation of Jiangsu Province (BK20140592), and the W.N. Keck Fundation.

Supporting information for this article is available on the WWW under http://dx.doi.org/10.1002/anie.201411040.

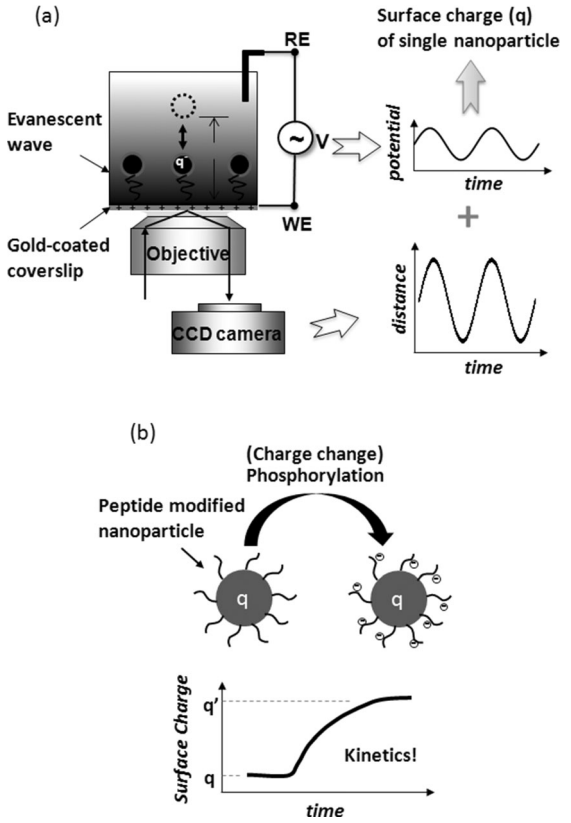

Figure 1. a) Illustration of the principle of nano-oscillator technology and b) its application in monitoring dynamic phosphorylation processes. a) A single nanoparticle with a negative surface charge *q* was driven to vertically oscillate with a periodic potential. A plasmonic imaging was utilized to measure the distance *d* between nanoparticle and Au-coated coverslip. The surface charge analysis on single nanoparticle trajectory and applied external field revealed the effective charge *q* of the nanoparticle. b) The phosphorylation of peptide molecules that were bound to Au nanoparticles increased the effective charge of peptide-modified nanoparticle. This dynamic process was monitored by the proposed plasmonic imaging method in real time, enabling the study on the kinetics of peptide phosphorylation.

linker is soft, so k is small. Also because the viscous damping is large, the inertia term, which is the first term of Equation (1) can be neglected, which leads to a simple relation between the measured oscillation amplitude, x_0, and the charge of the nanoparticle, given by Equation (2):

$$x_0 = \frac{E_0}{j12\pi^2\eta a f}q \qquad (2)$$

By measuring the oscillation amplitude, the charge of the individual nanoparticles can be determined if E_0, f, a, and η are known. For aqueous solution, $\eta = 9\times10^{-4}\,\mathrm{Ns\,m^{-2}}$, and a, the radius of the Au nanoparticles, is 20 nm, and f is the applied frequency. To obtain E_0, we measured the current density J, and determined E_0 from $E_0 = J/\sigma$, where σ is the conductivity of the solution.

To create an array of the nano-oscillators, a flexible molecule, HS-$(PEG)_n$-biotin (MW = 10000), was first self-assembled on the Au surface by the thiolate-Au bond. The surface was then exposed to streptavidin-modified 40 nm Au nanoparticles to allow them to link to the surface via the specific streptavidin–biotin interaction. The biotin-PEG linker was long (ca. 80 nm) and flexible such that the Au nanoparticles could oscillate with sufficiently large amplitude, which was measured for accurate determination of the charge of the nanoparticles. To ensure that each Au nanoparticle could bind only to a single biotin-PEG linker, the surface coverage of the PEG was diluted with short HS-$(PEG)_4$-OCH_3 spacer. The OCH_3 terminated PEG molecules also helped minimize non-specific attachments of the Au nanoparticles on the surface (see the Supporting Information).

After preparing the self-assembled nano-oscillators, a periodic potential was applied to the Au surface with a potentiostat to drive the nano-oscillators into oscillation. Consequently, the distance between the Au nanoparticle and the surface would change periodically with the applied potential, which was imaged by the plasmonic imaging microscope. Figure 2a shows the response of the nanoparticle-surface distance (solid line) for a typical nano-oscillator to a periodic potential with frequency of 10 Hz and amplitude of 0.1 V. The phase difference between the oscillation and applied potential is 180 degrees, indicating the nanoparticle was negatively charged. This observation was consistent with the negative zeta potential (−21 mV) of streptavidin-coated Au nanoparticle measured in the same solution (10 mM PBS). To confirm the observation, we varied the solution pH from 4 to 8, and found that the charge polarity changed to positive for pH lower than 5.0, which is close to the measured isoelectric point of surface-bound streptavidin (Figure 2b).[12]

The oscillation amplitude was linearly proportional to the potential amplitude when the amplitude was less than ca. 0.1 V, as predicted by Equation (2). However, further increasing the potential amplitude yielded smaller and smaller increase in the oscillation amplitude, eventually saturating at about 70 nm (Figure 2c). The saturation was due to the limited molecular length of the biotin-PEG linker, which was about 80 nm for PEG molecules with a molecular mass of 10 kDa. This observation was further supported by detailed analysis of the oscillation displacement due to a slowly varying potential. According to Equation (2), a slowly varying potential (or small f) would lead to large oscillation amplitude. Because the nanoparticles were tethered to the Au surface with the molecular linker, the oscillation amplitude could only reach a maximum value close to the length of the molecular linker, and the oscillation amplitude switched back and forth between zero (nanoparticles on the surface), and the length of the linker molecule (nano-oscillators are fully stretched). This behavior was indeed observed, as shown in Figure 2d.

To demonstrate the capability of the nano-oscillators for studying phosphorylation, we used SRCtide as a model peptide in the present work. SRCtide is a peptide containing 14 amino acid residues with the sequence GEEPLYWSFPAKKK. In the presence of kinase Src and ATP, the peptide is phosphorylated at its tyrosine residue.[13] To attach SRCtide to the nano-oscillators, we exposed the nano-oscillators self-assembled on the Au surface to biotinylated SRCtide to allow the binding of SRCtide to Au nanoparticles. Figure 3a shows a plasmonic image that reveals individual nano-oscillators,

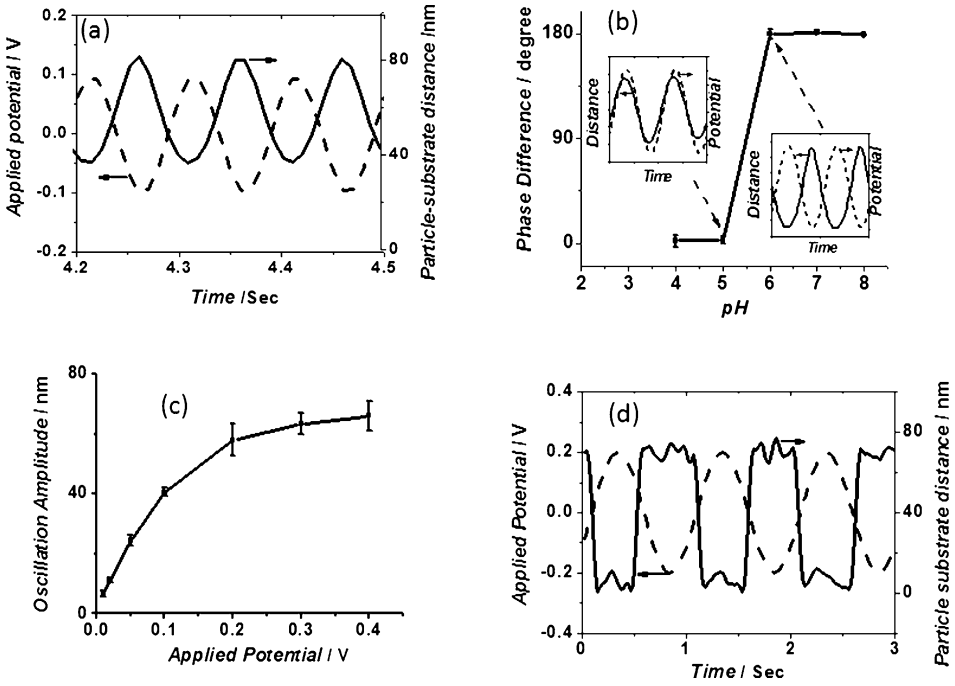

Figure 2. a) A nanoparticle oscillates (——) by responding to a periodic potential (-----) with certain phase difference, depending on the charge polarity of the nanoparticle. b) At a pH higher than 5.5, the distance between nanoparticle and substrate decreases with increasing applied potential, suggesting the nanoparticle is negatively charged. However, at a pH lower than 5.5, the distance increases with increasing potential, which is expected for positively charged nanoparticles. c) The oscillation amplitude initially increases with increasing potential before a plateau is reached. d) Stepwise up-and-down movement of nano-oscillators under higher potential and lower frequency. Solution: 10 mM phosphate-buffered saline (PBS).

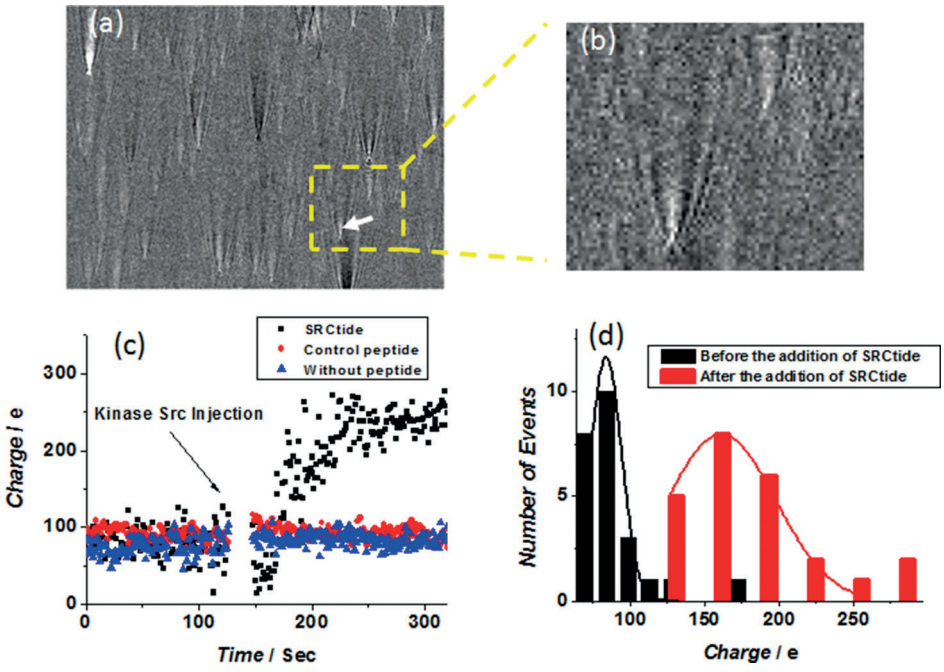

Figure 3. a) A typical plasmonic image consisting of tens of individual nano-oscillators. A zoomed image of a single nano-osillator is shown in (b). c) The effective charge change of SRCtide (black), control peptide (red) functionalized, and streptavidin-coated (blue) nano-oscillator before and after the injection of 6 nM kinase Src. Note that the gap after kinase injection was due to the turbulence of solution with manual kinase injection. d) Histogram distributions of effective charge of circa 30 nano-oscillators before (black) and after (red) phosphorylation. kinase buffer: 5 mM Mg^{2+}, 1 mM HEPES (pH 7.4), 0.4 mM ATP.

each as a bright spot with a parabolic tail (Figure 3b). The parabolic tail was produced by the scattering of the Au nanoparticle towards the surface plasmonic waves propagating on the surface.

From the measured oscillation amplitude, we first determined the charge of each nanoparticle before phosphorylation took place. The charge varied from one nanoparticle to another, and its distribution can be fitted with a Gaussian distribution with an average effective charge of 85 e (Figure 3d, black bars). By taking into account of ionic screening effect (64%) under the experimental conditions,[11] the average total charge of each nanoparticle is about 236 e. Because each surface-bound streptavidin has two negative charges at pH 7.4,[12a] the number of streptavidin molecules per nanoparticle was estimated to be 118. This result is consistent with a previous report in which 100 BSA molecules (similar in size) were usually observed on individual 40 nm Au nanoparticles.[14]

When kinase Src was added to the solution, the SRCtide could be phosphorylated in the presence of ATP, kinase Src, and Mg^{2+}, leading to more negative charge of the Au NPs. Black dots in Figure 3c show the charge change of an individual nano-oscillator marked by the white arrow in Figure 3a,b. Before phosphorylation, the nanoparticle had an effective charge of 80 e. At $t = 127$ s, kinase Src was injected into the buffer solution and equilibrated for 20 s. The charge of the nanoparticles was found to increase gradually and then reach a plateau of 245 e at $t = 250$ s. As a control, we carried out the experiment using nano-oscillators without functionalization of SRCtide, which did not show any detectable change in charge upon introduction of kinase Src (blue curve in Figure 3c). We also carried out an

additional control experiment with nano-oscillators functionalized with peptides that did not contain tyrosine residue, which did not show a change in charge either (red curve in Figure 3c). These control experiments indicated that the observed charge change in the SRCtide functionalized nanoparticles was due to phosphorylation (see the Supporting Information).

The successful phosphorylation of surface-bound SRCtide by kinase was also confirmed by measuring the zeta potential of SRCtide-functionalized Au nanoparticles before and after phosphorylation. The zeta potential of SRCtide-functionalized Au nanoparticles in the kinase buffer was determined to be −16 mV. Subsequently, SRC kinase was added to the Au nanoparticles functionalized with SRCtide and left for 2 h to complete the phosphorylation. The zeta potential after the phosphorylation was determined to be −20 mV. Meanwhile, no significant change in zeta potential was observed for Au nanoparticles functionalized with control peptide (Supporting Information, Figure S3). These results indicated that surface-bound SRCtide molecules were indeed phosphorylated in the presence of kinase.

There is a statistical distribution in the amount of phosphorylation-induced change in charge for different nanoparticles. The distribution follows a Gaussian distribution (Figure 3d, red bars), with an average charge of 163 e. The average effective charge associated with phosphorylation increased by 78 e, or a net increase of 217 e after considering the screening effect. Since adding a phosphate group increases the charge of peptide by 2 e at pH 7.4,[15] we estimated that the number of phosphorylated peptides is about 108. Because 118 streptavidin molecules were bound to single nanoparticle, the results suggest approximately 1 out of 4 biotin binding sites of streptavidin molecules were occupied during the biotylated SRCtide modification.

We further studied the kinetics of phosphorylation by varying kinase Src concentration from 0.2 to 6 nM (Figure 4a). The kinetics became faster with the kinase concentration, which is expected according to the model shown in Equation (3).[8c,16]

$$[E] + [S] \underset{k_-}{\overset{k_+}{\rightleftharpoons}} [ES] \xrightarrow{k_{cat}} [P] + [E] \quad (3)$$

where [E], [S], [ES], and [P] represent the concentration of enzyme, substrate, enzyme-substrate complex, and product, respectively. By fitting the kinetic data shown in Figure 4a with the above mode, we determined the reaction rate constant (K_{obs}), which increased linearly with the kinase concentration at low kinase concentrations, and then reached a plateau at high concentrations (Figure 4b). The result suggested a model of enzyme quasi-saturable system, according to previous studies on the enzymatic kinetics on solid substrates (see the Supporting Information).[16a] From the model, the Michaelis constant (K_m) and catalytic rate constant (k_{cat}) were estimated to be 0.85 nM and 0.013 s^{-1}, respectively.

In conclusion, we have developed a nano-oscillator method to study phosphorylation kinetics. Compared with the existing antibody-based approach, the present method does not require antibodies, and is label-free, thus capable of detecting phosphorylation without prior knowledge about phosphorylation sites, and measuring kinetic constants. Unlike many other label-free detection technologies (including SPR and QCM) that measure mass changes, the nano-oscillators detect changes in charge, making it particularly suitable for studying phosphorylation that involves a substantial charge change but a small mass change. The nano-oscillator platform is combined with plasmonic imaging, which provides high sensitivity for detection of a few phosphorylation events, and high spatial resolution for the simultaneous monitoring of many individual nano-oscillators in parallel.

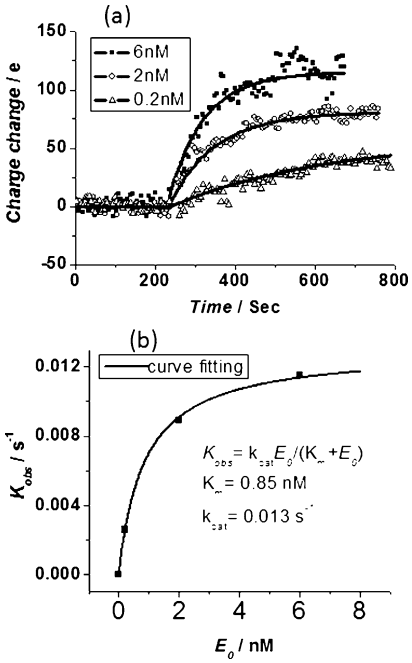

Figure 4. a) Dynamic change in the effective charge of nano-oscillators during the phosphorylation with different kinase Src concentration. △ 0.2 nM, ○ 2 nM, ■ 6 nM. b) The observed reaction rate constant (K_{obs}) increased with kinase concentration. Data points were obtained from the average of ca. 30 individual nano-oscillators.

Received: November 13, 2014
Published online: January 12, 2015

Keywords: charge-based detection · nano-oscillators · phosphorylation · plasmonic imaging · real-time imaging

[1] P. Cohen, *Nat. Cell Biol.* **2002**, *4*, E127–E130.
[2] a) P. Lahiry, A. Torkamani, N. J. Schork, R. A. Hegele, *Nat. Rev. Genet.* **2010**, *11*, 60–74; b) C. Kunick, I. Ott, *Angew. Chem. Int. Ed.* **2010**, *49*, 5226–5227; *Angew. Chem.* **2010**, *122*, 5354–5356; c) M. E. Breen, M. E. Steffey, E. J. Lachacz, F. E. Kwarcinski, C. C. Fox, M. B. Soellner, *Angew. Chem. Int. Ed.* **2014**, *53*, 7010–7013; *Angew. Chem.* **2014**, *126*, 7130–7133; d) P. Cohen, *Nat. Rev. Drug Discovery* **2002**, *1*, 309–315.
[3] a) J. S. Sebolt-Leopold, R. Herrera, *Nat. Rev. Cancer* **2004**, *4*, 937–947; b) J. M. Zhang, P. L. Yang, N. S. Gray, *Nat. Rev. Cancer* **2009**, *9*, 28–39; c) R. W. Hendriks, S. Yuvaraj, L. P. Kil, *Nat. Rev. Cancer* **2014**, *14*, 219–232.
[4] a) S. R. Datta, H. Dudek, X. Tao, S. Masters, H. A. Fu, Y. Gotoh, M. E. Greenberg, *Cell* **1997**, *91*, 231–241; b) D. H. Ebert, H. W.

Gabel, N. D. Robinson, N. R. Kastan, L. S. Hu, S. Cohen, A. J. Navarro, M. J. Lyst, R. Ekiert, A. P. Bird, M. E. Greenberg, *Nature* **2013**, *499*, 341 – 345.

[5] a) S. B. Ficarro, M. L. McCleland, P. T. Stukenberg, D. J. Burke, M. M. Ross, J. Shabanowitz, D. F. Hunt, F. M. White, *Nat. Biotechnol.* **2002**, *20*, 301 – 305; b) H. Marx, S. Lemeer, J. E. Schliep, L. Matheron, S. Mohammed, J. Cox, M. Mann, A. J. R. Heck, B. Kuster, *Nat. Biotechnol.* **2013**, *31*, 557.

[6] J. Homola, S. S. Yee, G. Gauglitz, *Sens. Actuators B* **1999**, *54*, 3 – 15.

[7] N. J. Cho, C. W. Frank, B. Kasemo, F. Hook, *Nat. Protoc.* **2010**, *5*, 1096 – 1106.

[8] a) A. Shoji, M. Kabeya, M. Sugawara, *Anal. Biochem.* **2011**, *419*, 53 – 60; b) K. Park, J. Ahn, S. Yeon, M. Kim, B. H. Chung, *Biochem. Biophys. Res. Commun.* **2008**, *368*, 684 – 689; c) H. Nishino, T. Nihira, T. Mori, Y. Okahata, *J. Am. Chem. Soc.* **2004**, *126*, 2264 – 2265; d) M. M. Orosco, C. Pacholski, M. J. Sailor, *Nat. Nanotechnol.* **2009**, *4*, 255 – 258.

[9] V. K. Lacey, A. R. Parrish, S. L. Han, Z. X. Shen, S. P. Briggs, Y. G. Ma, L. Wang, *Angew. Chem. Int. Ed.* **2011**, *50*, 8692 – 8696; *Angew. Chem.* **2011**, *123*, 8851 – 8855.

[10] a) W. Wang, K. Foley, X. Shan, S. P. Wang, S. Eaton, V. J. Nagaraj, P. Wiktor, U. Patel, N. J. Tao, *Nat. Chem.* **2011**, *3*, 249 – 255; b) S. P. Wang, X. N. Shan, U. Patel, X. P. Huang, J. Lu, J. H. Li, N. J. Tao, *Proc. Natl. Acad. Sci. USA* **2010**, *107*, 16028 – 16032; c) W. Wang, Y. Z. Yang, S. P. Wang, V. J. Nagaraj, Q. Liu, J. Wu, N. J. Tao, *Nat. Chem.* **2012**, *4*, 846 – 853.

[11] X. Shan, Y. Fang, S. Wang, Y. Guan, H.-Y. Chen, N. Tao, *Nano Lett.* **2014**, *14*, 4151 – 4157.

[12] a) S. Sivasankar, S. Subramaniam, D. Leckband, *Proc. Natl. Acad. Sci. USA* **1998**, *95*, 12961 – 12966; b) L. Almonte, E. Lopez-Elvira, A. M. Baró, *ChemPhysChem* **2014**, *15*, 2768 – 2773.

[13] T. J. Boggon, M. J. Eck, *Oncogene* **2004**, *23*, 7918 – 7927.

[14] a) S. Ju, W. S. Yeo, *Nanotechnology* **2012**, *23*, 135701; b) S. H. Hong, M. J. Kim, J. H. Ahn, W. S. Yeo, *Anal. Methods* **2013**, *5*, 3816 – 3818.

[15] a) E. S. Groban, A. Narayanan, M. P. Jacobson, *PLoS Comput. Biol.* **2006**, *2*, 0238 – 0250; b) J. T. Du, C. H. Yu, L. X. Zhou, W. H. Wu, P. Lei, Y. Li, Y. F. Zhao, H. Nakanishi, Y. M. Li, *FEBS J.* **2007**, *274*, 5012 – 5020.

[16] a) O. A. Gutiérrez, M. Chavez, E. Lissi, *Anal. Chem.* **2004**, *76*, 2664 – 2668; b) C. J. Gray, M. J. Weissenborn, C. E. Eyers, S. L. Flitsch, *Chem. Soc. Rev.* **2013**, *42*, 6378 – 6405.

